Twenty-Four Centrifuge Tests to Quantify Sensitivity of Lateral Spreading to Dr and PGA

Bruce L. Kutter¹; Trevor J. Carey²; Bao Li Zheng³; Andreas Gavras⁴; Nicholas Stone⁵; Mourad Zeghal⁶; Tarek Abdoun⁷; Evangelia Korre⁸; Majid Manzari⁹; Gopal S. P. Madabhushi¹⁰; Stuart Haigh¹¹; Srikanth S. C. Madabhushi¹²; Mitsu Okamura¹³; Asri Nurani Sjafuddin¹⁴; Sandra Escoffier¹⁵; Dong-Soo Kim¹⁶; Seong-Nam Kim¹⁷; Jeong-Gon Ha¹⁸; Tetsuo Tobita¹⁹; Hikaru Yatsugi²⁰; Kyohei Ueda²¹; Ruben R. Vargas²²; Wen-Yi Hung²³; Ting-Wei Liao²⁴; Yan-Guo Zhou²⁵; and Kai Liu²⁶

```
<sup>1</sup>Dept. of Civil and Environ. Eng., Univ. of California, Davis, CA 95616, U.S.
```

ABSTRACT

Twenty-four centrifuge model tests have been conducted at nine different geotechnical centrifuge facilities around the world as part of the international LEAP effort (liquefaction experiments and analysis projects). All of the centrifuge models represent a 4 m deep 5 degree sloping submerged sand deposit. The mean effective PGA of the input motion for all of the experiments was approximately 0.15 g and the mean relative density was approximately 65%, but the effective PGA's varied between about 0.07 g and 0.3 g, and the relative densities varied between about 40% and 75%. The test matrix was designed to enable experimental quantification

²Dept. of Civil and Environ. Eng., Univ. of California, Davis, CA 95616, U.S.

³Dept. of Civil and Environ. Eng., Univ. of California, Davis, CA 95616, U.S.

⁴Dept. of Civil and Environ. Eng., Univ. of California, Davis, CA 95616, U.S.

⁵Dept. of Civil and Environ. Eng., Univ. of California, Davis, CA 95616, U.S.

⁶Dept. of Civil and Environ. Eng., Rensselaer Polytechnic Institute, Troy, NY, U.S.

⁷Dept. of Civil and Environ. Eng., Rensselaer Polytechnic Institute, Troy, NY, U.S.

⁸Dept. of Civil and Environ. Eng., Rensselaer Polytechnic Institute, Troy, NY, U.S.

⁹Dept. of Civil and Environ. Eng., George Washington Univ., Washington, DC, U.S.

¹⁰Dept. of Engineering, Cambridge Univ., U.K.

¹¹Dept. of Engineering, Cambridge Univ., U.K.

¹²Dept. of Engineering, Cambridge Univ., U.K.

¹³Dept. of Civil and Environ. Eng., Ehime Univ., Matsuyama, Japan

¹⁴Dept. of Civil and Environ. Eng., Ehime Univ., Matsuyama, Japan

¹⁵Dept. of Geotechnique Eau et Risques, IFSTTAR, Bouguenais, France

¹⁶Dept. of Civil and Environ. Eng., Korean Advanced Inst. of Science and Tech., KAIST, Republic of Korea

¹⁷Dept. of Civil and Environ. Eng., Korean Advanced Inst. of Science and Tech., KAIST, Republic of Korea

¹⁸Dept. of Civil and Environ. Eng., Korean Advanced Inst. of Science and Tech., KAIST, Republic of Korea

¹⁹Dept. of Urban Systems Eng., Kansai Univ., Osaka, Japan

²⁰Dept. of Urban Systems Eng., Kansai Univ., Osaka, Japan

²¹Disaster Prevention Research Institute, Kyoto Univ., Kyoto, Japan

²²Disaster Prevention Research Institute, Kyoto Univ., Kyoto, Japan

²³Dept. of Civil Engineering, National Central Univ., Jhongli City, Taoyuan, Taiwan

²⁴Dept. of Civil Engineering, National Central Univ., Jhongli City, Taoyuan, Taiwan

²⁵Dept. of Civil Engineering, Zhejiang Univ., Hangzhou 310058, P.R. China

²⁶Dept. of Civil Engineering, Zhejiang Univ., Hangzhou 310058, P.R. China

of not only the median response but also the trend and sensitivity of the model response to density and shaking intensity. Quantification of the sensitivity of the response to initial conditions is a prerequisite for objective evaluation of the quality of the model test data. In other words, a discrepancy between two experiments should be evaluated after accounting for the uncertainty in the initial conditions and the sensitivity of the response to initial conditions. For the first time, a sufficient number of experiments has been performed on a similar problem to provide meaningful quantitative evaluation of the trend between PGA, density, and displacement. The sensitivity is quantified by the gradient of the trend and the uncertainty of the trend is quantified from the residuals between the fitting data and the trend.

INTRODUCTION

LEAP (Liquefaction Experiments and Analysis Projects) is an international effort to perform model tests to assess the accuracy of numerical procedures for predicting the effects of liquefaction. The present work follows on the planning phase of LEAP described by Manzari et al (2017) and Kutter et al. (2017).

Quantitative assessments of accuracy of a numerical procedure depend on knowing the accuracy and uncertainty of the reference experimental data. To understand the accuracy and uncertainty of the data, the inter-laboratory reproducibility of the experiments must be established. Since repeatability is not perfect, the assessment of differences between experiments should be interpreted with rigorous consideration of the variability of the initial conditions and boundary conditions and knowledge of the sensitivity of the results to the variations of the initial conditions. Some components of variability of the initial and boundary conditions can be measured, but additional variability is due to uncertainties in the measurements, as well as unknown variables. Rigorous assessment of numerical simulation procedures has many other prerequisites that are not addressed in the present paper (e.g., material properties calibration data, adequate constitutive models and numerical integration tools, and elimination of human error). Past validation efforts have sometimes focused on comparisons between predictions and experiments for a single data point. Duplication of a single data point can be deceptive: two uncorrelated functions can intersect to produce fortuitous duplication. Hence for LEAP we have attempted to produce sufficient data to enable definition of the trend between response parameters and key input parameters (relative density of the soil, intensity of shaking, and the frequency content of the shaking).

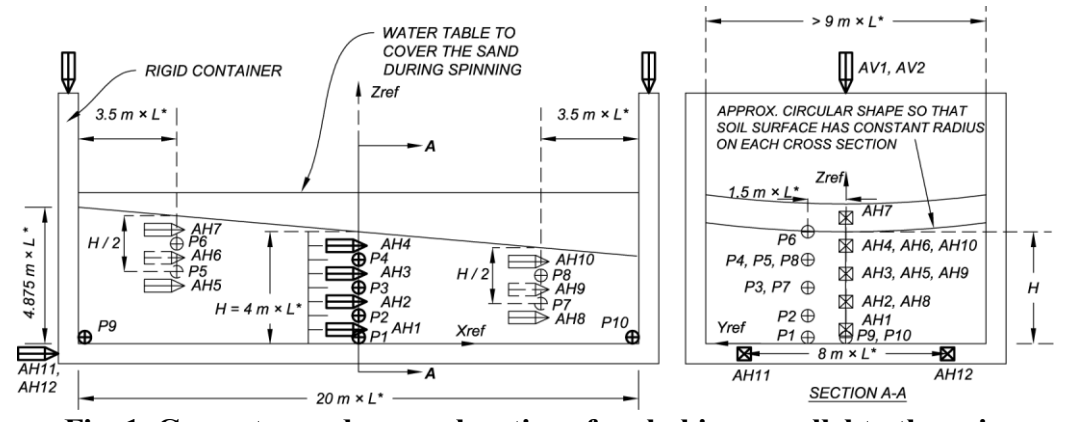


Fig. 1. Geometry and sensor locations for shaking parallel to the axis.

Twenty-four centrifuge models composed of uniformly pluviated Ottawa F-65 sand

represented 20 m long, 4 m deep submerged deposits with a 5° slope. The Ottawa F-65 sand, obtained from US Silica, Ottawa IL. UC Davis obtained a large shipment from US Silica and then shipped the sand to the facilities in Asia and Europe. RPI received a separate shipment of Ottawa F-65 sand, also in 2014.

The slopes were tested in nine different centrifuge facilities (see Table 1) in different sized rigid containers and instrumented with accelerometers and pore pressure sensors as illustrated in Fig. 1. Table 1 summarizes the scale factor, L* = (length in model)/(length in prototype) used in the present study, the radius of the centrifuge, the length to width of the rigid containers, and the shaking direction (some centrifuge shakers shake in the tangential direction and others shake parallel to the centrifuge axis) for each centrifuge facility. The surfaces of the models were specified to be curved to compensate for the radial g-field as indicated in Fig. 1 (section A-A) for models shaken parallel to the axis; for models shaken in the tangential direction, the curvature would have been apparent in the side view, but not in section A-A. Surface markers were also placed in a regular pattern to enable measurement of the surface displacements using hand measurements or photography before and after model earthquakes.

Table 1. Selected scale factor, shaking direction, centrifuge radius, and container shape.

Centrifuge Facility Institution	L*	Shaking Direction	Radius (m)	Container Length/Width
Cambridge University, UK	1/40	Tangential	3.56	2.1
Ehime University, Japan	1/40	Parallel to axis	1.184	4.1
IFSTTAR, France	1/50	Parallel to axis	5.063	2.0
KAIST, Rep. of Korea	1/40	Parallel to axis	5	2.2
Kyoto University, Japan	1/44.4	Tangential	2.5	3.1
National Central Univ., Taiwan	1/26	Parallel to axis	2.716	2.2
Rensselaer Polytechnic Inst., USA	1/23	Parallel to axis	2.7	2.4
Univ. of California Davis, USA	1/43.75	Tangential	1.094	1.6
Zhejiang University, China	1/30	Parallel to axis	4.315	1.7

To define the trend between liquefaction performance (e.g. lateral displacement or pore pressure ratio) and the key input parameters (e.g., the intensity of the input motion and the initial relative density), the input parameters were varied across the range indicated in Table 2. Fig. 2 plots the achieved PGA_{eff} (defined later) as a function of relative density for all of the experiments performed.

The first method of determining the density was by direct measurement of mass and volume of the model -- an approach that is deceptively difficult. Small errors due to sand mounding near the container side walls during pluviation, imperfect container rectangularity, uneven (rough) surfaces at the base and top of the sand deposit, as well as resolution and accuracy of the load cells used to measure the weight of the sand and the container contribute to the uncertainty of the mass and volume measurement. Also note that the relative density is very sensitive to density; at $D_r = 60\%$, a 1% error in density results in a 6% error in relative density. The maximum (1765 kg/m³) and minimum (1476 kg/m³) index densities were taken as the average values determined by more than 10 different teams.

The second method of determining relative density was to empirically correlate the density of the sand to the cone penetration tip resistance. All of the cone data used to produce the data in Table 2 were obtained from 6 mm diameter cone penetrometers. All of the cones, except the one used in Cambridge, were machined in the same machine shop at UC Davis and distributed to the

various facilities. A separate suite of experiments, described by Carey et al. (2018) showed that the Cambridge and Davis cones produced very similar results.

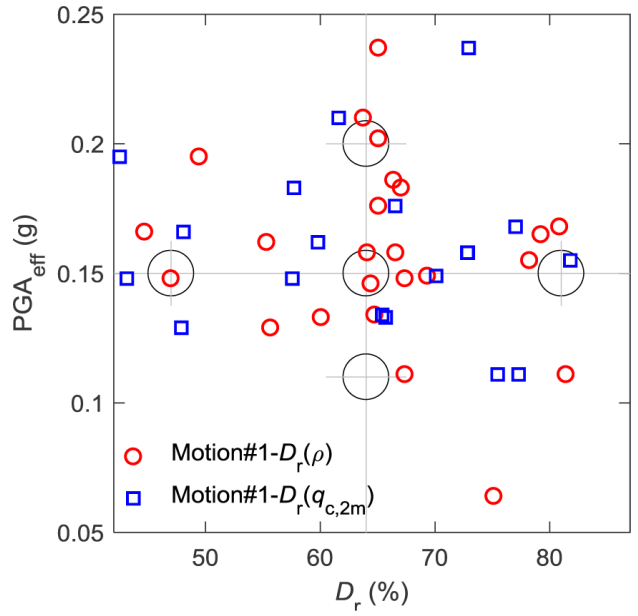


Fig. 2. Achieved PGAeff for motion#1 d relative density for all 24 model tests.

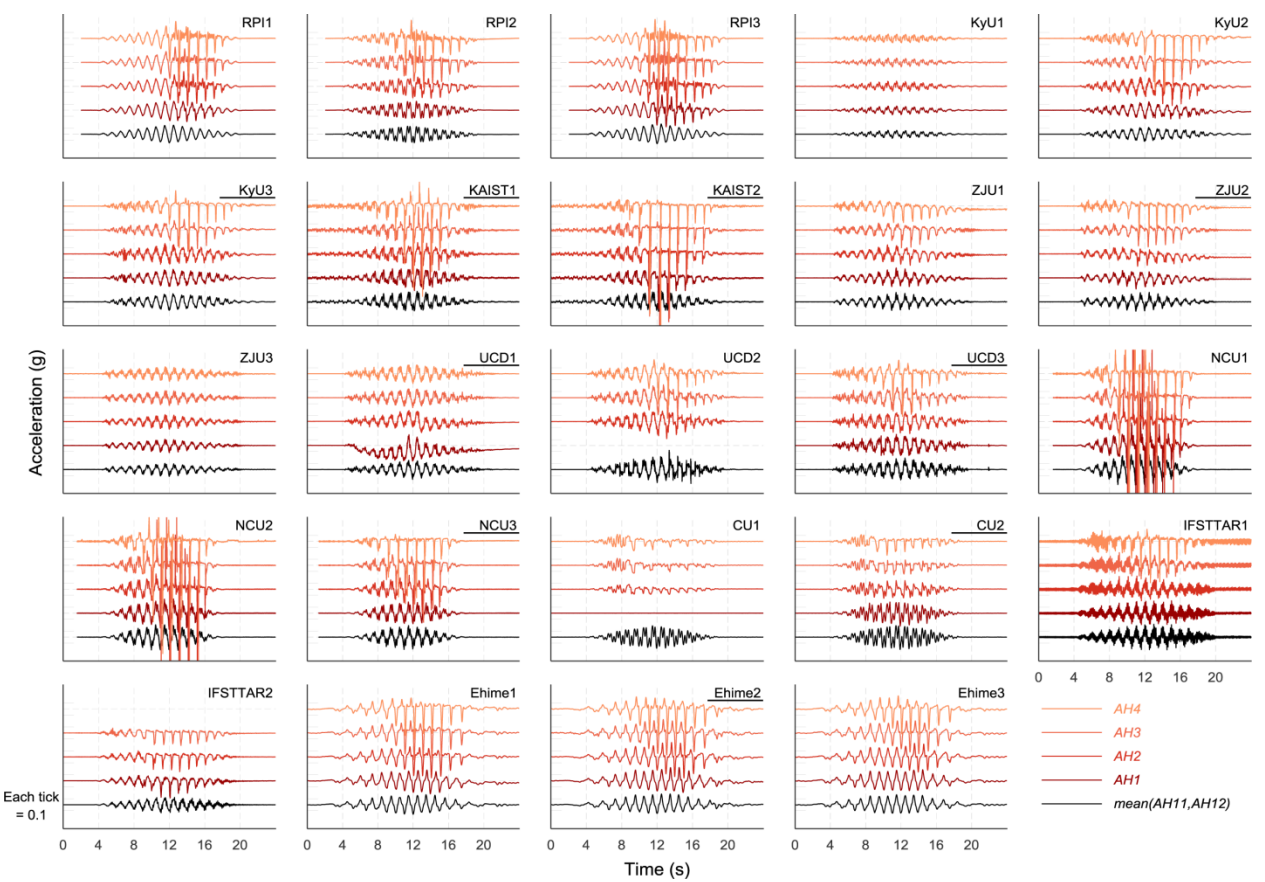


Fig. 3. AH4, AH3, AH2, AH1 and base acceleration for the first destructive shaking event for 24 model tests.

A custom correlation between measured density and cone tip resistance at a depth of 2 m was obtained by linear least squares fit from all of the available LEAP model tests. The linear correlation was then used to obtain the density from the tip resistance. The obtained correlation was likely influenced by the layer thickness, the lateral stress, and stress history, and possibly the centrifuge model scale factor. The obtained relationship is very similar to that presented by Carey et al (2018), except that additional data was used for the present study.

RESULTS

The mean of the base accelerations recorded by AH11 and AH12 are plotted as the bottom trace of each subplot in Fig. 3; the peaks of these traces are summarized as PGA in Table 2. The main component of the target ground motion in each case is a 16 cycle, 1 Hz motion with a linearly tapered amplitude such that the PGA occurred in the middle cycle. The main component shape is very similar to the base motion recorded for RPI1 or KyU2 (see Fig. 3). As is apparent in Fig. 3, each centrifuge shaker imposed additional high frequency components superimposed on the tapered sine wave motion. It was reasoned that short period acceleration pulses would have smaller peak velocities and would have less effect on the model than would the acceleration pulses with long period. As a first approximation, the PGA_{eff} was obtained by finding the amplitude of the 1 Hz component of the input motion and adding to that half the peak amplitude of the higher frequency components of the motion: $PGA_{eff} = PGA_{1Hz} + 0.5 * PGA_{HF}$. The procedure for determining PGA_{1Hz} and PGA_{HF} is PGA1PPis described in more detail by Kutter et al. (2017).

Acceleration Time Series Data: Fig. 3 shows the base acceleration and the accelerations recorded by the central vertical array (AH1-AH4 in Fig. 1). Three of the experiments (KyU1, ZJU3, and UCD1) show almost uniform acceleration behavior – in other words, the models behaved like a rigid body – a clear indication that liquefaction did not occur in these experiments. All of the other experiments showed significant nonlinear behavior and evidence of liquefaction. The sharp downward spikes, most significant in AH3 and AH4, we call "dilation spikes" because they are caused by the sudden increase in effective stress and hence increase in stiffness associated with negative pore water pressures produced by the tendency of the sand to dilate as in response to the imposition of large shear strains. The spikes are larger in the downward direction because this corresponds to shearing in the down-slope direction; strains tend to accumulate in the downslope direction. The presence of these spikes is a good indicator of liquefaction.

Comparing the characteristics of the input base motion, Fig. 3 shows that the base motion for test UCD2 contains some large amplitude sharp spikes, IFSTTAR1 has more continuous high frequency components, and CU1, CU2, and RPI2 contain significant 3 Hz components superimposed on the motion. RPI2 motion was intentionally varied to allow emulation of the high frequency component observed in the CU experiments. The first few and last few cycles of the motion produced by the Ehime shaker are lower frequency than 1 Hz; this is a nuance of their mechanical shaker.

Some aspects of the recorded data are obviously influenced by faulty instrumentation. For example, the data from AH3 and AH4 in UCD1 show almost uniform behavior, similar to the base acceleration, indicating very little deformation of the soil; therefore, it is clear that the offset seen in AH1 and to a lesser extent AH2 are anomalous and probably due to an instrumentation issue. AH1 is not reported for UCD3, and AH1 is not reported for IFSTTAR2. AH1 appears to be nonfunctional (flat) in CU1.

Table 2. Key Strength-Demand-Performance Parameters

Table 2. Key Strength-Demand-1 error mance 1 arameters								
Test ID	D _r from mass and volume	D _r from q _c at 2 m depth	PGA (g)	PGA _{eff} (g)	Peak cyclic relative displacement (mm)	Avg. lateral disp. of 2 central markers, Ux2 (mm)		
CU1	0.66	0.41	0.190	0.186	66	440		
CU2	0.49	0.43	0.206	0.195	56	490		
Ehime1	0.64	0.73	0.169	0.158	47			
Ehime2	0.67	0.73	0.180	0.158	61	100		
Ehime3	0.78	0.82	0.168	0.155	55	60		
IFSTTAR1	0.79	-	0.214	0.165	32	50		
IFSTTAR2	0.56	0.48	0.135	0.129	40^{3}	438		
KAIST1	0.81	0.77	0.178	0.168	37	2		
KAIST2	0.45	0.48	0.185	0.166	63	0		
KyU1	0.75	-	0.071	0.064	1	<u> </u>		
KyU2	0.67	0.75	0.119	0.111	40	150		
KyU3	0.60	0.66	0.143	0.133	44	0		
NCU1	0.65	0.73	0.292	0.237	113	287		
NCU2	0.65	-	0.224	0.202	79	256		
NCU3	0.65	0.67	0.217	0.176	54	279		
RPI1	0.64	-	0.150	0.146	45	93		
RPI2	0.67	0.58	0.144	0.148	61	132		
RPI3	0.55	0.60	0.170	0.162	72	126		
UCD1	0.69	0.70	0.165	0.149	4	0		
UCD2	0.64	0.62	0.339	0.21	47	125		
UCD3	0.67	0.58	0.192	0.183	51	160		
ZJU1	0.65	0.65^2	0.167	0.134	35	135		
ZJU2	0.47	0.43	0.191	0.148	46	263		
ZJU3	0.81	0.77^2	0.135	0.111	2	30		

¹The surface marker data from KyU1 and KyU2 are not reliable and hence are not reported.

Based upon the response recorded by the upper accelerometers (AH3 and AH4) CU1 shows the most severe isolation of the ground surface motion associated with liquefaction; towards the end of the earthquake record, the surface motion is almost flat. Other surface records that show severe spikes or isolation are Kaist2, ZJU2, NCU1, NCU2, NCU3, CU2, IFSTTAR2 and Ehime1. Consistent with this, all of these events also produced permanent displacements larger than 250 mm (see Table 2).

As mentioned earlier, three of the experiments (KyU1, ZJU3, and UCD1) show almost uniform acceleration behavior – a clear indication that liquefaction did not occur in these experiments. It is interesting to note the computed peak cyclic relative displacement between the ground surface and the base motion was less than 4 mm for these 3 experiments (see Table 2). The peak cyclic relative displacement (given in prototype scale) was computed by double integration of the difference between AH4 and the base acceleration.

²ZJU3 CPT profile was extrapolated from about 1.7 to 2.0 m to enable computation of Dr(qc(2m)).

³For IFSTTAR2, the peak cyclic displacement was obtained from the difference between AH3 and AH_{base}.

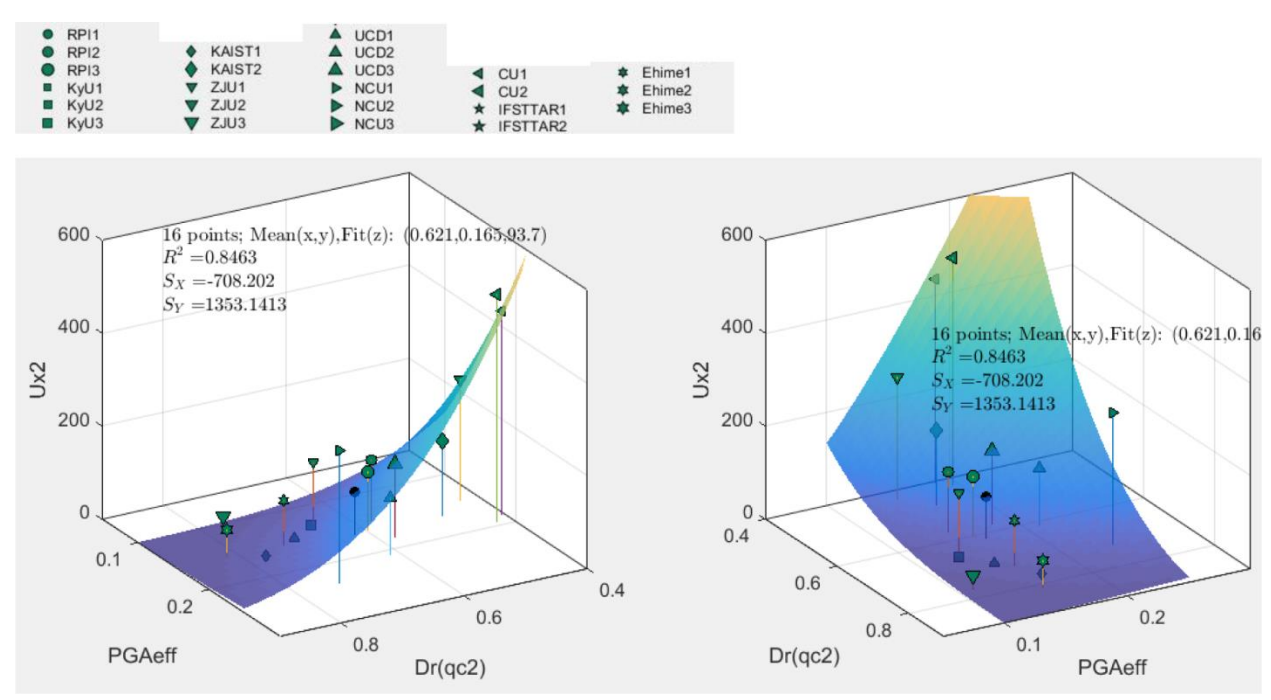


Fig. 4. Two views of the correlation between permanent displacement, PGA_{eff} , and relative density (Dr(qc2)) obtained from the cone resistance at 2 m depth for 16 of the 19 tests that provided all of this information. Three outliers were excluded. Note that R^2 is 0.846.

Comparison of Permanent Displacements: Table 2 lists the permanent lateral displacement, Ux2, determined by the averaged movement at the two central surface marker locations before and after the first destructive shaking event. In most cases, Ux2 was obtained by hand measurement of surface markers using a caliper before and after spinning the centrifuge; in some cases, the surface marker displacements were also measured by image analysis of data from high speed cameras. The permanent displacements are primarily a function of the intensity of shaking and the relative density of the sand.

Fig. 4 shows a 3-D plot of lateral displacement, Ux2, as a function of PGA_{eff} and Dr(qc2), the relative density determined from the measured qc at mid-depth (2 m) and the regressed relationship between density and tip resistance at mid-depth. Four experiments did not report cone penetration results at 2 m depth, so only 19 experiments could be presented in this type of plot. For Figure 4, however, three experimental results that may be "outliers" were excluded from the analysis and this produced a very large coefficient of correlation between the data and the surface obtained by nonlinear regression, $R^2 = 0.846$. The equations used for the linear regression are described later. For Fig. 5, the same analysis produced $R^2 = 0.578$ when all 19 points were included in the regression analysis; none of the "outliers" were excluded. It is interesting that removing 3 data points has a significant effect on the correlation coefficient.

Also shown in Fig. 5 is a plot of the residuals between the fitted surface and the measured displacement data Residual(Ux2), as a function of PGAeff and $D_r(qc2)$. From studying the residuals plot, it appears that the function used for the curve fitting did not produce an obvious pattern of residuals; i.e., there is no convincing pattern showing that residuals tend to be larger in some regions than in other regions of the space. This is one indication that the fitting function is suitable for fitting this data set.

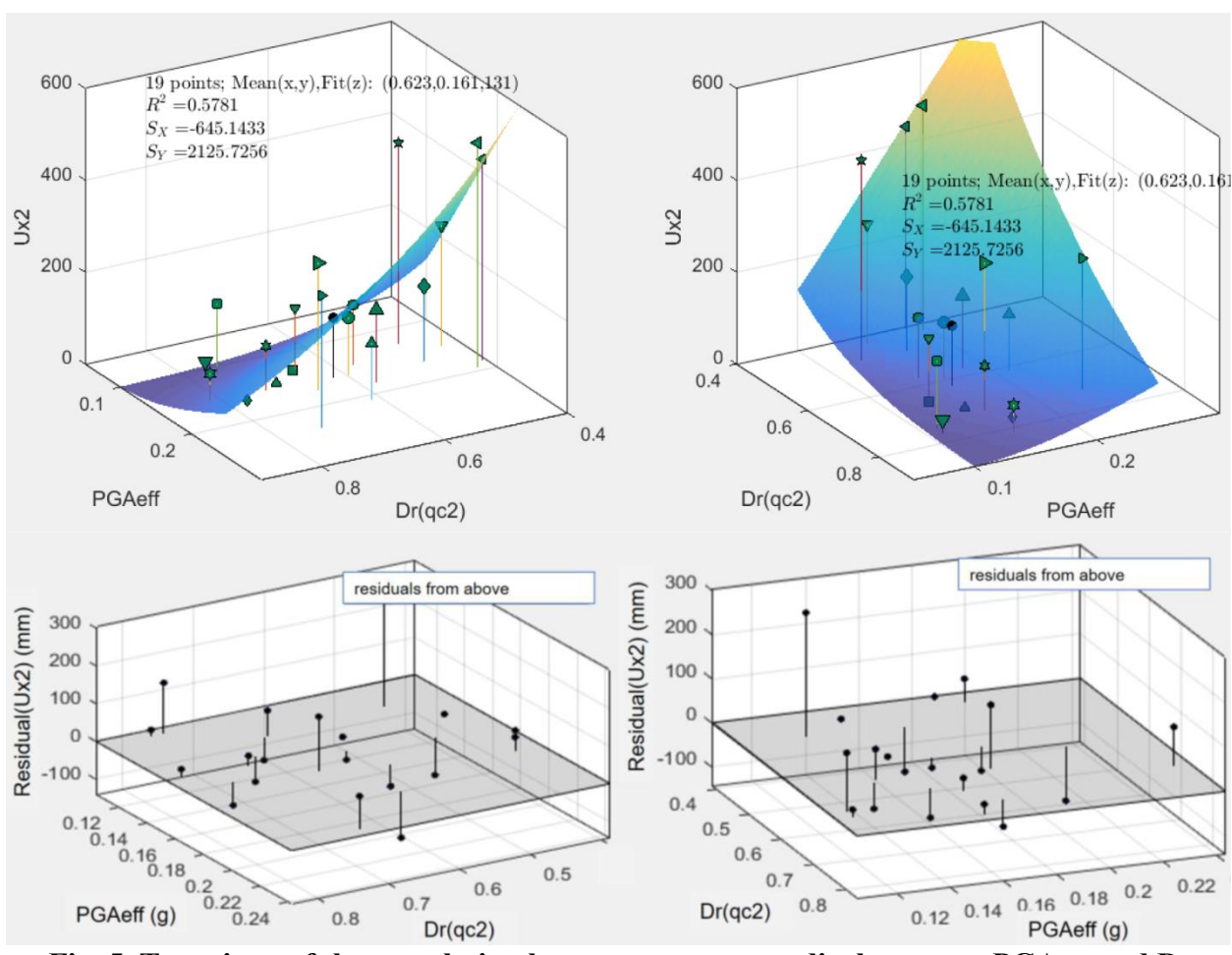


Fig. 5. Two views of the correlation between permanent displacement, PGA_{eff} , and D_r obtained by correlation between density and cone resistance at 2 m depth. Note that 19 tests provided all of this information. R^2 for this curve fit is 0.578. The bottom plots show the residual displacement between the fitted surface and the experimental data.

By comparing the data presented in Table 3 for Fig. 4 (R²=0.86) and Fig. 6 (R²=0.60), one may judge that the correlation degrades when the relative density is based upon mass and volume measurements instead of the cone penetration resistance. This suggests that Dr(qc(2 m)) is more consistent than Dr(mass and volume measurements). Considering that the quality of the correlation improves when outliers are neglected, both Fig. 4 and Fig. 6 excluded three or four outliers, though Fig. 6 does contain three more data points in total. By comparing the data presented in Table 3 for Fig. 4 (R²=0.86) and Fig. 7 (R²=0.48), one may judge that the correlation degrades when PGA is used as the intensity measure instead of PGA_{eff}.

As described earlier, PGAeff uses a 50% weighting factor for the high frequency components of the input motion and a 100% weighting factor for the lower frequency components of the input motion. It appears that this preliminary method of accounting for the effects of frequency content does a decent job of accounting for some effects of the differing frequency contents. More rigorous methods to account for the frequency effects on the performance should be developed.

The filled black circle data point in each of Figs. 4-7, is plotted at the mean of the PGA and D_r values for the analyzed data set, with the z-coordinated determined by evaluation of the

regression surface at the mean PGA and D_r . As expected, the black circle plots exactly on the surface. At this mean point, the gradient of the surface was also evaluated; the gradient of the surface, S_x , can be considered to be a measure of the sensitivity of displacement to D_r in units of mm. Similarly, S_y is a measure of the sensitivity of displacement to PGA in units of mm/g. For direct comparison, the sensitivities S_x and S_y are summarized in Table 3. While the values of S_x and S_y do vary depending on the intensity measure and method to quantify D_r , the data set does provide some meaningful information regarding both the median performance and the sensitivity of the performance to variations in the initial conditions.

The shape of the symbols in Figs. 4-7 indicate the institution that produced the data and the size of the symbols is different for each test as indicated in the legend above Fig. 4.

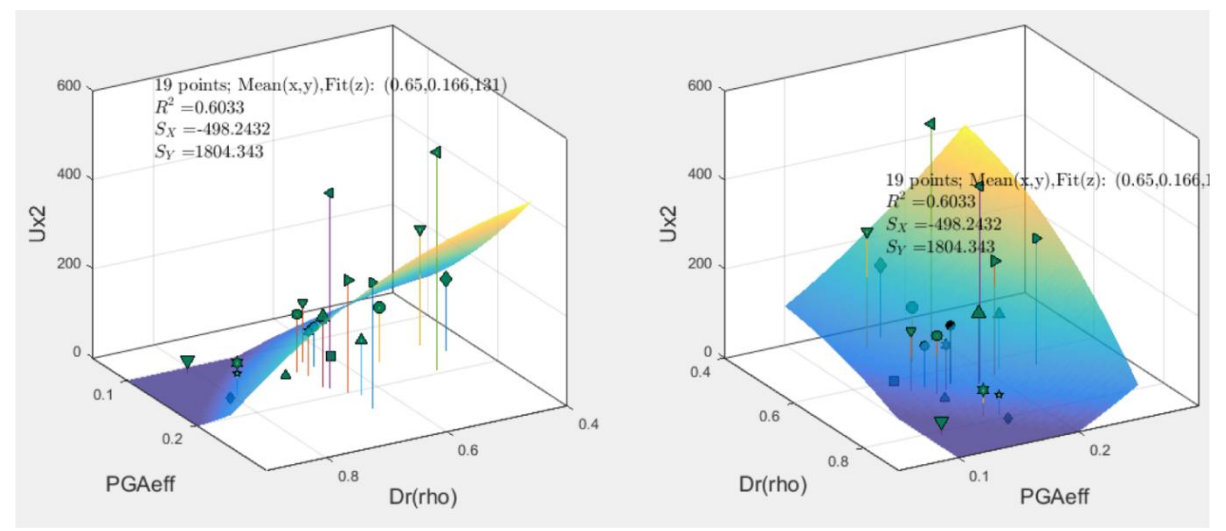


Fig. 6. Two views of the correlation between permanent displacement, PGA_{eff} , and $D_r(rho)$ obtained directly from mass and volume measurements when 4 outliers are excluded. Note that R^2 for this curve fit is 0.603.

Table 3. Summary of results from regression analysis.

Case	Motion	Basis to	Data	Correla	Sensitiv-	Sensitiv	Mean Dr, mean
	Intensity	determine	Points	tion	ity to Dr	-ity to	IM, and
	Measure	D_{r}	Used /	Coef.	at mean	IM at	evaluation of
	(IM)		Excluded	\mathbb{R}^2	(mm)	mean	curve fit at mean
	(g)		outliers			(mm/g)	(g, 1, mm)
Fig. 4	PGA _{eff}	q _c (2 m)	16/3	0.846	-708	1356	0.62, 0.165, 94
Fig. 5	PGA _{eff}	q _c (2 m)	19 / 0	0.578	-645	2125	0.62, 0.161, 131
Fig. 6	PGA _{eff}	Mass &	19 / 4	0.603	-492	1804	0.65, 0.166, 131
		Vol.					
Fig. 7	PGA	$q_c(2 m)$	19 / 0	0.485	-829	611	0.62, 0.185, 154

DESCRIPTION OF THE REGRESSION SURFACE USED TO FIT THE DATA

The shape of the surface used to perform then regression was loosely based on curves presented by Yoshimine et al. (2006). Idriss and Boulanger (2008) approximated the Yoshimine et al curves by:

$$\gamma_{max} = 0.035(2 - FS_{liq}) \frac{1 - F_{\alpha}}{FS_{liq} - F_{\alpha}}$$
 (1)

Where $FS_{liq} = CRR/CSR$ is the factor of safety with respect to triggering of liquefaction and F_{α} is a function of relative density. Note that equation 1 is not applicable if FS_{liq} is greater than 2, and would return a strain potential, γ_{max} of zero for $FS_{liq} = 2$. The curve fit equation used for displacement for this study was:

$$Ux = b_2 b_1 - \frac{(D_r - 0.125)^{n_3} + 0.05}{1.3 \frac{a_{max}}{g}} \left(\frac{a_{max}}{g}\right)^{n_2} (1 - D_r)^{n_4}$$
 (2)

Where the second term inside the Macauley brackets $\langle \rangle$ is meant to be analogous to FS_{liq} and the b1 term corresponds to the constant, 2, in equation 1. Note that $\langle x \rangle = x$ if x > 0; $\langle x \rangle = 0$ if x < 0. However, for the present study, coefficients b_1 , b_2 , n1, n2, n3, and n4 are determined by nonlinear regression. Inclusion of the term in Macauley brackets, with the restriction that $0.125 < D_r < 1$, produces a smooth function and prevents this function from producing not-physically-realistic uphill residual displacements. As an example, the curve fit parameters determined using a nonlinear regression algorithm in Matlab that produced the surface plotted in Fig. 4 are: $b_1 = 12$, $b_2 = 0.0456$, n1 = 4.57, n2 = 1.157, n3 = 1, and n4 = 2.

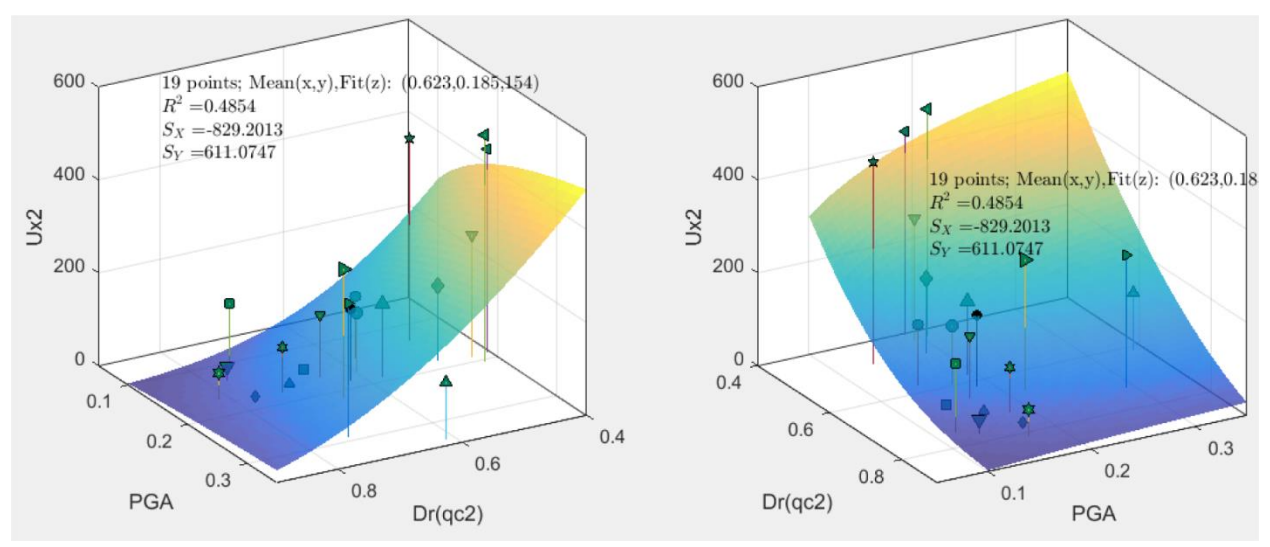


Fig. 7. Two views of the correlation between Ux2, PGA, and D_r determined from cone penetration resistance. Note that R² is 0.485.

CONCLUSIONS

This paper presents the trend observed between lateral spreading displacements, the effective PGA, and the relative density for the first destructive motion of twenty-four experiments performed at nine different centrifuge facilities. Different methods of quantifying the input motion and relative density are evaluated by performing nonlinear regression. Cone penetration tests were performed on most of the centrifuge models. It is found that using correlations between lateral displacement, relative density based on CPT resistance, and PGA_{eff} provided better correlation coefficients than correlations between lateral displacement, relative density based on volume and mass measurements, and PGA.

The LEAP coordinated study provides, for the first time, data from a sufficient number of experiments to begin to quantify the trend between displacement, relative density, and motion intensity for a lateral spreading problem. Quantifying this trend enables an improved understanding of the accuracy of the displacement and the sensitivity of the displacement to the input parameters. This quantification is an important prerequisite for assessing the repeatability of (or conversely, the significance of discrepancies between) the LEAP experiments.

ACKNOWLEDGEMENTS

The authors from various countries each received financial support from various agencies. The work at GWU, RPI, and UC Davis was supported by NSF Awards CMMI 1635307, CMMI 1635524 and CMMI 1635040. The work of Yan-Guo Zhou and Kai Liu was partly supported by the National Natural Science Foundation of China (Nos. 51578501, 51778573), the National Program for Special Support of Top-Notch Young Professionals (2013) and the Zhejiang Provincial Natural Science Foundation of China (No. LR15E080001).

REFERENCES

- Carey, T., Gavras, A., Kutter, B., Haigh, S.K., Madabhushi, S.P.G., Okamura, M., Kim, D.S., Ueda, K., Hung, W.-Y., Zhou, Y.-G., Liu, K., Chen, Y.-M., Zeghal, M., Manzari, M. (2018). A new shared miniature cone penetrometer for centrifuge testing, *Proc. Int. Conf. on Physical Modelling in Geotechnics*, ICPMG, London, July, In Press.
- Idriss, I.M. and Boulanger. R.W. (2008). *Soil Liquefaction During Earthquakes*, MNO-12, Earthquake Engineering Research Institute, p.142.
- Kutter, B. L., Carey, T. J., Hashimoto, T., Zeghal, M., Abdoun, T., Kokkali, P., Madabhushi, S. P. G., Haigh, S. K., Burali d'Arezzo, F., Madabhushi, S. S. C., Hung, W-Y., Lee, C-J., Cheng, H-C., Iai, S., Tobita, T., Ashino, T., Ren, J., Zhou, Y-G., Chen, Y., Sun, Z-B and Manzari, M. T. (2017). LEAP-GWU-2015 Experiment Specifications, Results, and Comparisons, *Journal of Soil Dynamics and Earthquake Engineering*, Elsevier, https://doi.org/10.1016/j.soildyn.2017.05.018.
- Manzari, M.T., El Ghoraiby, M., Kutter, B.L. Zeghal, M., Abdoun, T., Arduino, P., Armstrong, R.J., Beaty, M., Carey, T., Chen, Y., Ghofrani, A., Gutierrez, D., Goswami, N., Haigh, S.K., Hung, W-Y., Iai, S., Kokkali, P., Lee, C.-J., Madabhushi, S.P.G., Mejia, L., Sharp, M., Tobita, T., Ueda, K., Zhou, Y., Ziotopoulou, K. (2017). Liquefaction experiment and analysis projects (LEAP): Summary of observations from the planning phase, *Soil Dynamics and Earthquake Engineering*, 2017, ISSN 0267-7261, https://doi.org/10.1016/j.soildyn.2017.05.015.
- Yoshimine, M., Nishizaki, H., Amano, K., and Hosono, Y. (2006). Flow deformation of liquefied sand under constant shear load and its application to analysis of flow slide in infinite slope, *Soil Dynamics and Earthquake Engineering*, Vol. 26, pp. 253-264.